

Predicting critical machining conditions using time-series imaging and deep learning in slot milling of titanium alloy

Faramarz Hojati, Bahman Azarhoushang

Institute of Precision Machining (KSF) – Furtwangen University
hofa@hs-furtwangen.de
aza@hs-furtwangen.de

Abstract. Tool wear and tool breakage cause product damage in terms of low surface quality and undesired geometrical and dimensional tolerances, followed by a dramatic increase in the production cost. In this study, an Artificial Intelligence (AI) model has been developed to predict the critical machining conditions concerning surface roughness and tool breakage in the slot milling of titanium alloy. The signals recorded from the main spindle and different axes through the Siemens SINUMERIK EDGE Box integrated into a CNC machine tool were converted into images using Gramian Angular Field (GAF). Further, the converted images were used for training Convolutional Neural Network (CNN). The combination of GAF and trained CNN model indicates good performance in predicting critical machining conditions, particularly in the case of an imbalanced dataset.

Keywords: Artificial Intelligence, Gramian Angular Field, Convolutional Neural Network, Slot-milling, Edge Box, Imbalanced dataset.

1 Introduction

The cutting tool breakage or severe tool wear causes low product quality and damage to machine components. Therefore, the tool must be changed before these unwanted events. However, the tool cost increases with earlier tool changes. To avoid quality failure by changing the cutting tool at an appropriate time interval, the tool and process condition should be monitored using different sensors integrated into the machine tool [1]. In recent years, extensive research works have been conducted to monitor the cutting tool condition during the process for optimizing tool lifespan [2], early detection of tool wear, and prevention of tool breakage [3]. Direct monitoring of the cutting tool, which measures the tool geometry using vision or optical apparatus, requires expensive equipment and cannot be applied in real-time due to the presence of coolant and the contact between the tool and material [4]. Therefore, the focus of research activities was mainly on indirect approaches of tool and machining condition monitoring, which benefit from the fact that a variation in cutting tool condition changes certain variables such as cutting forces, vibration, and surface finish. In these methods, the current or power signals from the machine elements (like spindle or axis motors) [5,6] or signals from the sensors integrated into the machine tool (like piezosensor, accelerometer, strain gauge, thermocouple or acoustic emission sensor) [7–9] are analyzed to recognize the possible correlations with the cutting tool and machining condition.

The tool and process condition monitoring methods, generally need to extract the features of measured signal to use them for the model training. In this regard, the application of the utilized algorithm in the extraction of features varies from signal to signal, and the feature extraction requires a well-experienced person. Moreover, some information on the signal through the feature extraction would be lost. To solve this issue, imaging the signals using different approaches like Gramian Angular Field rather than feature extraction can be helpful. As an example, Arellano et al. [10] applied GAF for tool wear classification. The recorded cutting force signals were encoded to several images that have been used for training Convolutional Neural Network (CNN) classification model. A percentage of accuracy over 80% was reported for different groups corresponding to different states of tool wear (break-in, steady-state, and failure).

A need for analyzing the signal for process monitoring is growing with a new generation of machine tools capable of recording different types of data. The Siemens SINUMERIK EDGE (SE) Box that can be integrated into the machine tool record the signals from different axes and main spindles and fuse all measured data into a JSON file. The signals for recording are selected in the MindSphere Capture4Analysis application, which is connected with SINUMERIK EDGE Box. The current study aims to predict the machining condition using different types of signals recorded by the SINUMERIK EDGE Box integrated into the five axes CNC machine tool (Haas-Multigrind® CA). The experimental tests were conducted in milling a titanium alloy (Ti6Al4V) as a difficult-to-cut material. Severe tool wear and even tool breakage due to Built-Up Edge (BUE), particularly at high-speed machining of the titanium alloy, followed by low workpiece surface quality, was detected. After

measuring signals, GAF, as one of the time series imaging methods, was applied for encoding the signals into images. Further, images were used for training the CNN classification model to predict the critical machining condition. Eventually, the combination of the GAF and CNN model was evaluated.

2 Experiment

In this investigation, Ti6Al4V was selected as the workpiece material. Slot-milling was used as a milling strategy. The milling tests were carried out with different process parameters. In all tests, the axial depth of cut a_p was kept constant and equal to 1 mm, and the radial depth of cut a_e was 3 mm. The feed per tooth, f_z , and cutting speed v_c were considered as varying parameters. Figure 1a illustrates the experimental setup. The milling tool moved from the right side to the left side of the workpiece (according to the milling direction shown in Figure 1a), and for the creation of slots with a depth of 6 mm, six slot-milling passes each with axial depth of cut, a_p , of 1 mm were conducted. 161 tests (each test including 6 slot milling passes) were carried out with different combinations of varying process parameters. The tests were conducted with and without coolant lubricant. In the presence of cooling, no tool wear and tool breakage were observed. Therefore, several tests were also carried out without coolant lubricant (dry cutting) at the higher range of feeds and cutting speeds to increase the tool wear rate and reduce the required experimental time. Table 1 provides the range of milling parameters.

Table 1. Process parameters

Cutting speed v_c [m/min]	Feed per tooth f_z [$\mu\text{m}/\text{tooth}$]	Radial depth of cut a_e [mm]	Axial depth of cut a_p [mm]	Coolant
50-113	17-50	3	1	Oil / Dry

Figure 1b indicates the integration of the whole data acquisition system into the utilized milling machine. A five axes CNC machine tool (Haas-Multigrind® CA) with a Siemens controller was used in this study. For the data acquisition, the machine tool is equipped with a so-called Siemens SINUMERIK EDGE (SE) Box. Siemens CNC controls supply data, and SE makes it possible to record data and states of the control in a resolution of 1 ms (1kHz) parallel to the process. The SE box is, in principle, an industrial computer and has the corresponding resources to store the data. The MindSphere Capture4Analysis application enables the selection of the signals to be recorded and the trigger time from which a signal is to be recorded. The types of signals that Edge-Box for the main spindle and each axis can record are categorized into current, load, torque and power. At each milling pass, the Edge-Box started to automatically record the signals slightly prior to the slot milling process and the recording was automatically stopped after the cutting process. According to a defined system, the data is written to a JSON file on the hard disk of the SE box with the execution of the NC program. With a correspondingly high number of milling attempts, hundreds or thousands of files can be created. Further, the JSON File for each test is processed through a written ETL program (Extract-Transform-Load) to obtain the tabular data in CSV format. The CSV data and post-process information from the measurement system collected in tabular data are imported directly into Artificial Intelligent (AI) Model. Moreover, the CSV data can also be visualized using an external computer for the machine tool user.

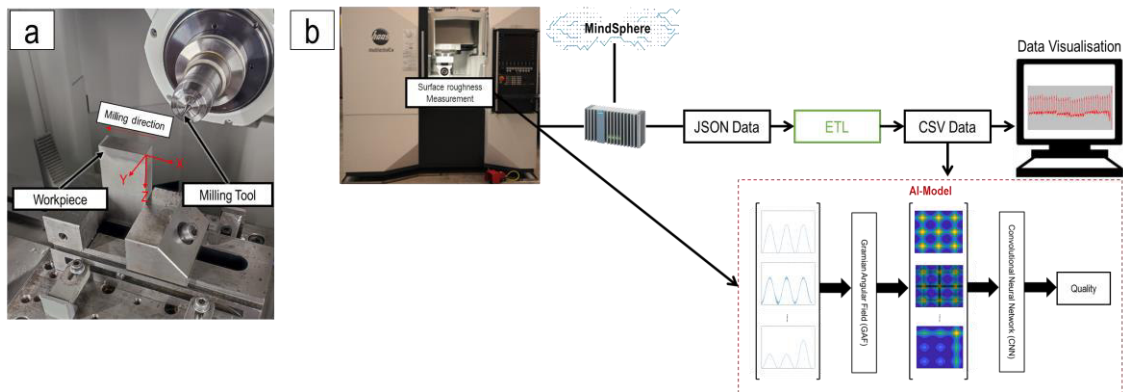


Fig. 1. (a) experimental setup (b) schematic representation of the integration of the ETL program and AI Model

The concept of the utilized AI Model is shown in Figure 1b. Instead of using the signals features such as mean, peak and standard deviation, each signal was converted into an image by Gramian Angular Field (GAF), which

contains all the features as well as the relationships between different points of the signal. In the next step, the images were used as input parameters for training the CNN model. Finally, the model can predict the quality of the process concerning the critical machining condition in terms of machined surface roughness and tool breakage with respect to new images obtained from new signals (even with different process parameters).

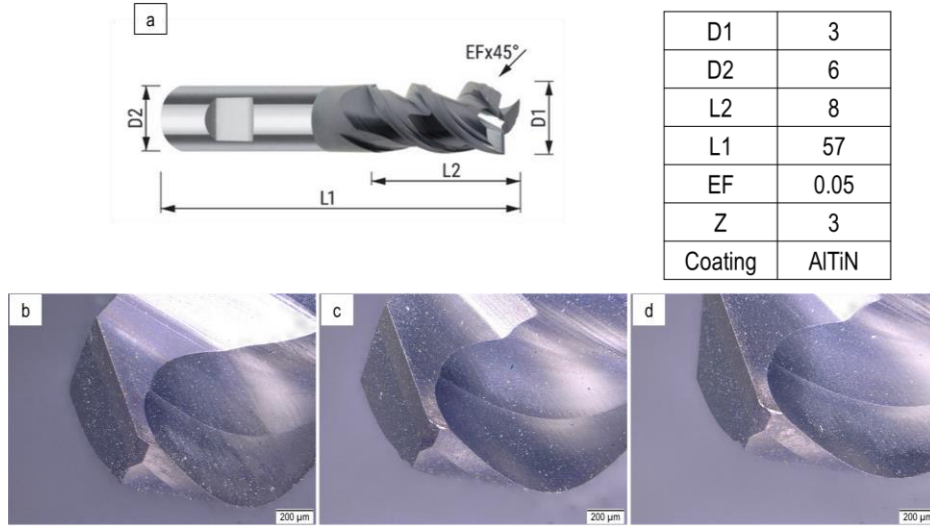


Fig. 2. (a) specification of utilized cutting tool (b) edge 1 (c) edge 2 (d) edge 3

Figure 2a shows the geometrical properties of the utilized tools. The milling tools were coated with AlTiN. D1, D2, L1, L2, EF and Z are cutting tool and shank diameter, total length, cutting edge length, corner chamfer and the number of teeth, respectively. Figure 2 (b-d) also demonstrated three cutting edges of a new tool.

3 Signal selection

According to the recorded signals, it was concluded that the signals in the z-axis for current, load and torque are the best candidates for the model training. In detail, the signals in other axes showed no remarkable change before tool breakage, while the mentioned types of signals in the z-axis considerably altered. Figure 3 illustrates an example of these signals before the tool breakage. After the second pass, a considerable fluctuation in all types of the signal can clearly be observed. This can be associated with considerable Built-Up Edge (BUE) at the dry milling of titanium alloys that was eventually followed by tool breakage. Since the response of three different types of signals (current, load and torque) are similar, using all of them for training the model is not required. Therefore, the load signal was used for further analysis. Figure 4 shows a considerable BUE at $v_c = 80$ m/min and $f_z = 20.6$ $\mu\text{m}/\text{tooth}$ that led to cutting edge and tool breakage.

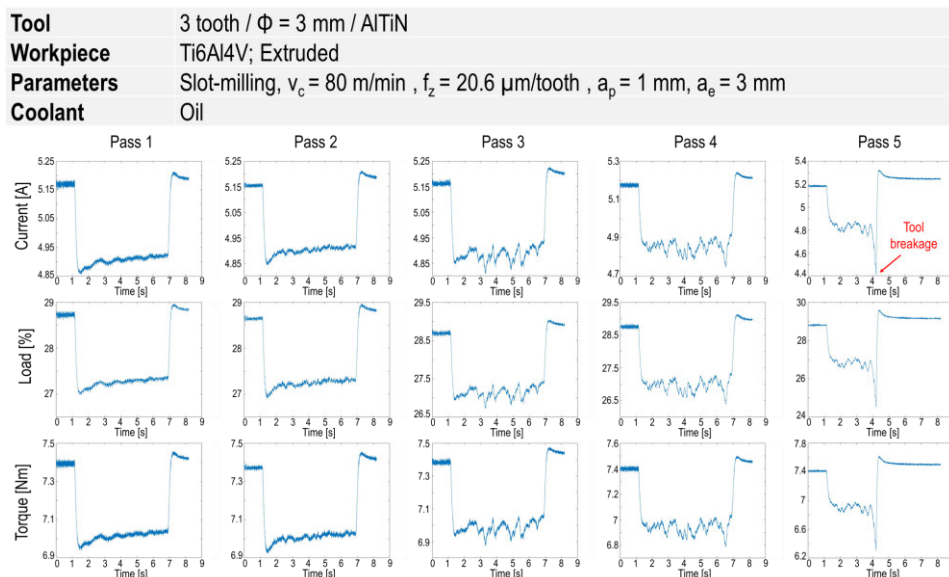


Fig. 3. Signals of Current, Load and Torque in different passes before tool breakage at $v_c = 80$ m/min and $f_z = 20.6$ $\mu\text{m}/\text{tooth}$

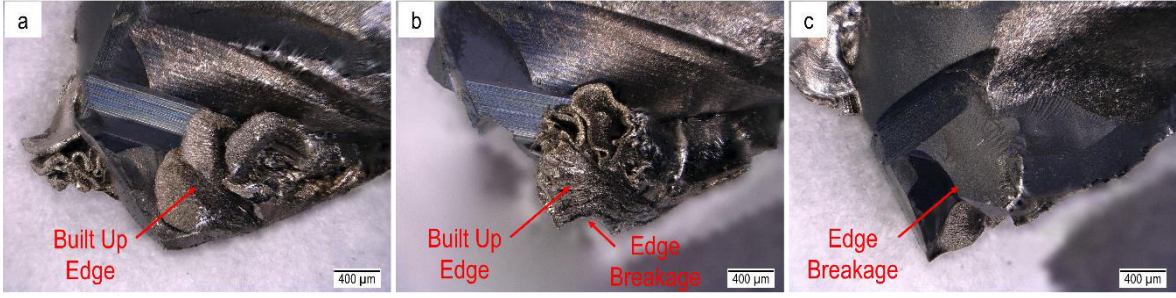


Fig. 4. BUE and Tool breakage at $v_c = 80$ m/min and $f_z = 20.6$ $\mu\text{m}/\text{tooth}$ (a) edge1 (b) edge2 (c) edge3

4 Gramian Angular Field (GAF)

The **GAF** algorithm encodes the time-series signal into an image, resulting in transferring the signal to a polar coordinate space. Using Gramian Angular Summation Field (**GASF**), the trigonometric sum is applied to each couple of angular positions of each time series point and the rest of the signal points for generating each row of the GASF matrices. Therefore, the temporal correlation between each point of the signal and the rest of the signal is calculated at each row as below:

$$\text{GASF} = \begin{bmatrix} \cos(\theta_1 + \theta_1) & \cdots & \cos(\theta_1 + \theta_n) \\ \cos(\theta_2 + \theta_1) & \cdots & \cos(\theta_2 + \theta_n) \\ \vdots & \ddots & \vdots \\ \cos(\theta_n + \theta_1) & \cdots & \cos(\theta_n + \theta_n) \end{bmatrix} \quad (1)$$

Figure 5 provides the corresponding GASF images of the signals for a series of 5 pass-milling before the tool breakage. At the first two passes, no remarkable change in the image (and correspondingly the row signals) can be observed, while afterwards, a dramatic change in images (alteration in the colors and pattern of images) associated with the signal fluctuation can clearly be seen that is followed by the tool breakage in the 5th pass.

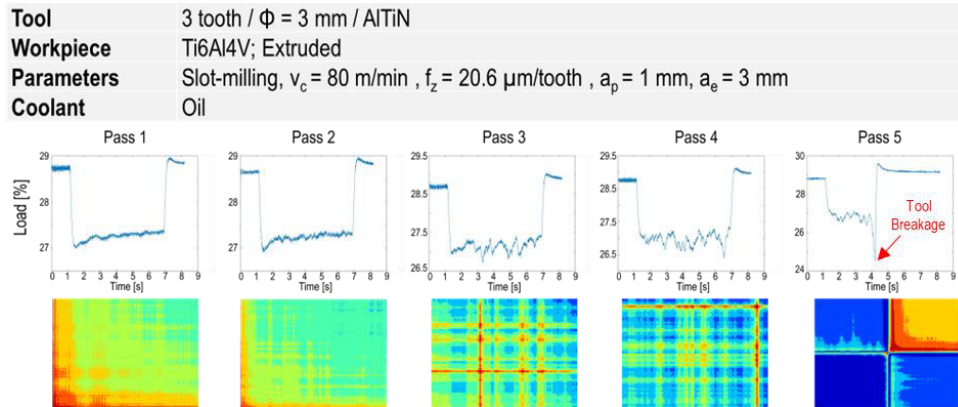


Fig. 5. GASF images at five different milling passes with a new tool at constant process parameters

5 Clustering

Before training the CNN model, the images were clustered into two main groups (A and B). Group A includes images of the tests where no tool breakage occurred, and acceptable surface quality was induced. Group B contains all images belonging to the experimental tests where tool breakage occurred, or the surface quality deteriorated dramatically. Figure 6a and Figure 6b indicate respectively the quality of milled surface associated with group A and group B and their corresponding GASF images. 858 GASF images were produced in this study. Based on the assumption regarding the clustering of images in two groups, 726 and 132 images corresponded to group A and group B, respectively.

Tool	3 tooth / $\Phi = 3$ mm / AlTiN
Workpiece	Ti6Al4V; Extruded
Parameters	Slot-milling, $v_c = 50$ and 75 m/min , $f_z = 22$ and 30 $\mu\text{m}/\text{tooth}$, $a_p = 1$ mm, $a_e = 3$ mm
Coolant	Oil / Dry

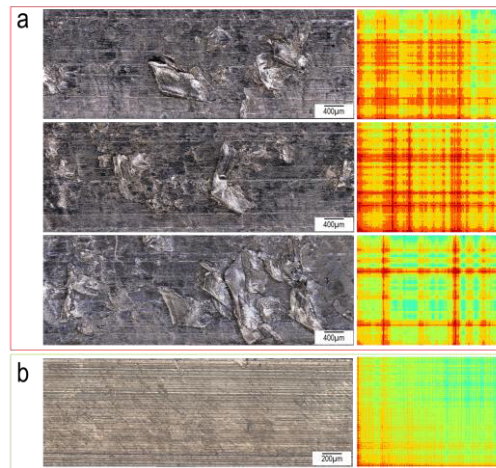


Fig. 6. Exemplary milled surfaces and their corresponding GASF images (a) at $v_c = 75$ m/min and $f_z = 22$ $\mu\text{m}/\text{tooth}$ in dry machining and (b) at $v_c = 50$ m/min and $f_z = 30$ $\mu\text{m}/\text{tooth}$ with oil

6 Convolutional Neural Network (CNN)

A Convolutional Neural Network (CNN), a commonly applied method for machine learning of images, was used as a classification model in this study. Figure 7 illustrates the architecture of the developed CNN model. Two main components in this model are the convolution layer and the pooling layer. In the convolution layer, multiple filters are applied to the imported image. Each filter scans the entire image, and at each position, the similarity of the filter is compared with that area of the image. The output of the Convolution Layer results in several images that are smaller than the original image. The number of images corresponds to the number of applied filters. In the next step, the Pooling Layer is applied to reduce the size of the images and, correspondingly, the number of parameters to be learned as well as the number of computations performed in the network. Moreover, the pooling layer extracts the most important features of the image. Therefore, the images are imported from the convolution layer to the pooling layer, which results in a dimension reduction while preserving the important features of the images. Finally, the images are flattened and imported into the neural network for training.

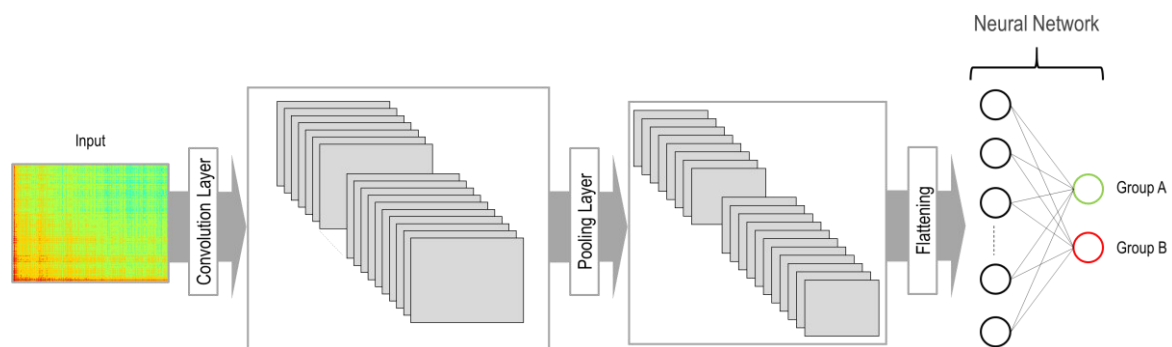


Fig. 7. Architecture of the CNN model

After creating the images using the GASF method, they are resized to 224×224 for importing into the CNN model. In this study, two convolution layers were determined. The number and size of filters for each convolution layer accounted for 128 and 3×3 , respectively. After each convolution layer, a pooling layer is placed with a pool size of 2×2 . Therefore, the imported images (with the size of 224×224) after the first convolution layer are reduced to 222×222 . Further, 128 images obtained from the first convolution layer are further subjected to the pooling layer, which results in 128 images with the size of 111×111 . Afterwards, the output of the second convolution layer results in images with the size of 109×109 . By applying the second pooling layer, the size of 128 images is eventually reduced to 54×54 . The Rectified Linear Unit (ReLU) function is applied as an activation function at both convolution and pooling layers. In the next step, two layers

in a neural network are determined. The number of neurons at the first and second layers accounted for 256 and 2, respectively. Due to binary classification, the sigmoid function is used as an activation function in the last layer.

7 Model evaluation

To evaluate better the trained model, the K-fold cross-validation approach was used. In this method, the dataset was divided into K groups, where K-1 groups are used for the training model and one group is used for the test. Again, the test group is changed, and the rest of the dataset is used for training. This procedure is repeated K times, and the average accuracy is considered as a good indicator for the future prediction of the model. In this study, K is set to 4 so that the data set for group A and group B has been divided into four groups. As mentioned before, the number of images in group A and B are 726 and 132, respectively. For each round of training, 545 and 181 images for group A are used for training and testing, respectively. In the case of group B, the number of images for training and testing accounted for 99 and 33, respectively.

Due to this fact that the accuracy is not a good indicator for model evaluation in the case of imbalanced dataset, other approaches such as Receiver Operator Characteristic (ROC) and Precision-Recall curves were used to evaluate a binary classifier for testing each group. For generating these curves, True Positive Rate (TPR) against False Positive Rate (FPR) and Precision versus Recall are plotted at various threshold values determined for sigmoid function in the last layer of the neural network. The calculation of Precision, Recall, TPR and FPR with respect to the confusion matrix are provided in Figure 8a. The classifier that provides a curve close to the top-left corner indicates a better performance based on the ROC curve. According to Figure 8b, the trained model at K = 2 shows better performance compared to others. The lowest performance concerning the ROC curve can be seen for K = 4. According to Figure 8c, it is desired that the classifier model has higher precision and recall. Therefore, the Precision-recall curve closer to the top-right corner shows better performance. Correspondingly, the trained model classifier at K = 1, 2, and 3 performed better than that at K = 4. A variation in performance of the trained model in different groups (K = 1, 2, 3 and 4) shown in Figure 8b and Figure 8c is related to the imbalanced dataset issue that the model is mainly trained by group A rather than group B. Figure 8d and Figure 8e illustrate the ROC curve and Precision-Recall curve, respectively, after oversampling the dataset through the image augmentation technique by ImageDataGenerator from the KERAS library at Python. Accordingly, a variation between curves has been reduced, and the Classifier at different groups indicates good performance. This highlighted the issue of the imbalanced dataset in the training of the model. Therefore, the extension of the dataset, particularly for group B, is important to assist the model training by reducing a degree of imbalance in the dataset.

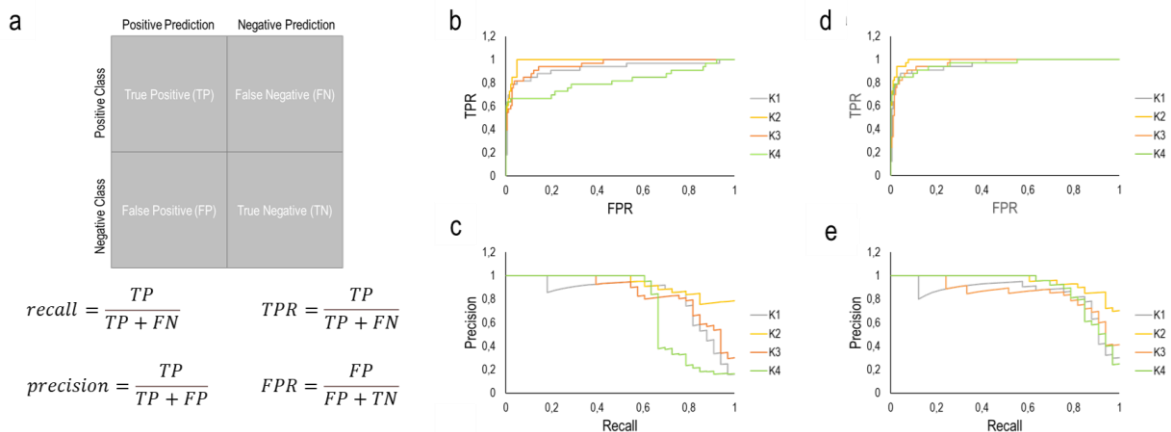


Fig. 8. (a) confusion matrix (b) ROC curve (c) Precision-Recall curve (d) ROC curve after oversampling (e) Precision-Recall curve after oversampling

8 Conclusion

In this study, the Gramian Angular Field (GAF) method was applied after collecting the process signals through an Edge computing device (Siemens SINUMERIK EDGE (SE) Box) integrated into the machine. The captured signals were encoded into images using GAF. Additionally, a CNN classification model was developed to predict the critical process conditions in milling a titanium alloy (Ti6Al4V). The developed AI model was able

to predict the critical process conditions in terms of tool breakage and low surface quality in the slot milling of Ti6Al4V even in the presence of an imbalanced dataset. The improvement of the model in the future can be carried out using expanding the dataset, particularly for collecting more experimental data associated with the critical machining condition.

References

1. Ambhore, N., Kamble, D., Chinchankar, S., Wayal, V.: Tool Condition Monitoring System: A Review. *Materials Today: Proceedings* 2(4-5) (2015) 3419–28
2. Teti, R., Jemielniak, K., O'Donnell, G., Dornfeld, D.: Advanced monitoring of machining operations. *CIRP Annals* 59(2) (2010) 717–39
3. Mohanraj, T., Shankar, S., Rajasekar, R., Sakthivel, NR., Pramanik, A.: Tool condition monitoring techniques in milling process — a review. *Journal of Materials Research and Technology* 9(1) (2020) 1032–42
4. Nouri, M., Fussell, BK., Ziniti, BL., Linder, E.: Real-time tool wear monitoring in milling using a cutting condition independent method. *International Journal of Machine Tools and Manufacture* 89 (2015) 1–13
5. Patra, K., Jha, AK., Szalay, T., Ranjan, J., Monostori, L.: Artificial neural network based tool condition monitoring in micro mechanical peck drilling using thrust force signals. *Precision Engineering* 48 (2017) 279–91.
6. Drouillet, C., Karandikar, J., Nath, C., Journeaux, A-C., El Mansori, M., Kurfess, T.: Tool life predictions in milling using spindle power with the neural network technique. *Journal of Manufacturing Processes* 22 (2016) 161–8
7. Zhang, XY., Lu, X., Wang, S., Wang, W., Li, WD.: A multi-sensor based online tool condition monitoring system for milling process. *Procedia CIRP* 72 (2018) 1136–41
8. Hesser, DF., Markert, B.: Tool wear monitoring of a retrofitted CNC milling machine using artificial neural networks. *Manufacturing Letters* 19 (2019) 1–4
9. Siddhpura, M., Paurobally, R.: A review of chatter vibration research in turning. *International Journal of Machine Tools and Manufacture* 61 (2012) 27–47
10. Martínez-Arellano G, Terrazas G, Ratchev S. Tool wear classification using time series imaging and deep learning. *Int J Adv Manuf Technol* 104(9-12) (2019) 3647–62